Case study on aircraft tyre wear in Y12 aircraft tyres

K. A. Dulani Daminda Kuruppu
dkuruppu1985@yahoo.com
C. J. Hettiarachchi
Department of Aeronautical Engineering
Faculty of Engineering
General Sir John Kotelawala Defence University
Ratmalana
Sri Lanka

ABSTRACT

The primary objective of this research was to analyse the discrepancies in polymeric properties in Y12 aircraft tyres after 50 landings. Tensile strength and elongation test, abrasion test and hardness tests were carried out for the nose and main gear tyres after the completion of 50 landings. Surface morphologies of the tyre samples were observed using SEM. ISO specifications were followed for each experimental method during testing. There was a reduction in both median tensile strength and elongation at break in aircraft tyres after 50 landings but the reduction rate of both parameters were lower in Tyre 2 (nose wheel tyre) compared with Tyre 1 (left main wheel tyre) and Tyre 3 (right main wheel tyre). The highest percentage of mean volume loss was reported for Tyre 3 (3.88%). In addition, the least percentage of mean volume loss was obtained in Tyre 2 (2.98%). The percentage of hardness reduction was highest in Tyre 2 (6.9%). The surface roughness was induced to the tyre surface after completion of 50 landings.

Keywords: Aircraft tyres; wear; polymeric properties

NOMENCLATURE

d   diameter
Wrs   weight loss with respect to (w.r.t.) the reference material
Ws   weight of the sample tyre
Wr   weight of the reference tyre sample, $Wr = 214.7\,\text{mg}$
D   mean density of the tyre samples, $D = 1.1428\,\text{g/cm}^3$

ABBREVIATIONS

ISO   International Organization for Standardization
NASA   National Aeronautics and Space Administration
NDT   Non-Destructive Testing
SEM   Scanning Electron Microscope

1.0 INTRODUCTION

Many safety studies on automobile tyres have been performed whereas only a few on aircraft tyres. The operating conditions and the structure of aircraft tyres are much more different tyrewhen compared to automobile tyres[1]. Basically, aircraft tyres are made out of a specific combination of rubber compounds, cord and steel belts. The major parts of an aircraft tyre are the body, sidewalls, beads, and treads[1]. Aircraft tyres require more attention compared to automobile tyres as aircraft tyres encounter sudden high speeds and heavy weights[2]. For safety in an aircraft, tyres play a major role during the taxiing and landing processes[3]. During the taxiing of an aircraft, tyres enable the aircraft to achieve the required speed to take off; while during landing, tyres provide a gripping surface, absorb initial loads, discharge electricity and also bear the weight of the aircraft.

Consider the rotational mechanism of aircraft tyres. The aircraft tyres first contact the runway and the wheels do not rotate at ground speed at that moment. This generates a speed difference between the translational ground speed of the aircraft and the tangential speed of the tyre radius, which causes the tyres to skid. By accelerating, the pilot can avoid the slipping of the wheels when the speed of the wheels matches the forward speed of the aircraft along the runway[4]. The small cloud of smoke can be visualised at the exact touchdown point during landing of the aircraft due to high friction between the runway surface and the tyre surface. This friction generates a high amount of heat which can even burn the tyre[5]. The polymeric properties of the polymers in the aircraft tyres are susceptible to degradation in the presence of high temperature. Hence, the aircraft tyres may lose their strength when they undergo high-temperature conditions[6].

As per the literature[7], most of the studies related to pneumatic tyres are about car tyres. Out of these studies, only a few research works were found for aircraft tyres. Three of these research studies were done by NASA[8–10] and they considered only the influence of temperature on aircraft tyres. When determining the thermomechanical behaviour of aircraft tyres, the researchers mustdeal with such nonlinearity parameters as geometry, the properties of the aircraft tyre materials, the friction coefficient, the dissipative mechanisms, and the thermal coefficients[11]. But it is very challenging to analyse those parameters as aircraft tyres experienced different operational and environmental conditions while in service[12]. Moreover, many attempts were taken to quantify tyre wear theoretically by aggregating the abrasion patterns, slippage, temperature effects and the geometry of the contact surface. But there is no

literature which was related to tyre wear in Y12 aircraft tyres. The primary objective of this research was to analyse the discrepancies in polymeric properties of nose and main-gear tyres in Y12 aircraft after completion of 50 landings. The outcome of this research work would help solve the lack of knowledge about the materials properties in aircraft tyres.

2.0 METHODOLOGY

In this study, polymeric properties were analysed in the nose and main-gear tyres of Y12 aircraft after the completion of 50 landings. Polymeric properties in each tyre sample was measured using three testing methods, namely Uniaxial tensile test and elongation test, Abrasion test and Hardness test. The ISO standards were followed throughout the testing process in order to obtain the most accurate results for each sample. The tyres have worn out only on one side of the tyre along the perimeter, while the other half along the perimeter was not worn out at all. During the selection process of the control tyre samples for the study, several concerns were made such as it was not appropriate to select a brand new tyre as a control tyre sample as it is stored under specific conditioning temperatures whereas experimental tyres are not. Because the objective of this study was to analyse the discrepancies in polymeric properties that occurred in the Y12 aircraft tyre after the completion of 50 landings; hence the control sample also should have gone through similar environmental and operational conditions. Hence, the unworn side of the aircraft tyres were taken as the control tyre samples to do the comparison of polymeric properties.

2.1 Selection of samples for the experiment

The landing gear configuration of Y12 aircraft is the non-retractable tricycle type with a single wheel in each nose gear and two main gears[13]. Three tyre samples were separately mounted to the nose gear, to the right main gear and also to the left main gear simultaneously. However, during the landing process, the main two gears support most of the weight of the aircraft compared with the nose gear, as the centre of gravity is forward of the main gear. Aircraft are usually designed to carry 10–12% of the aircraft weight on the nose gear and 88–90% distributed equally between or among the main gears[14]. Hence, the three tyre samples were not subjected to the same loads. But the total weight of the aircraft with the passengers was maintained constant during every landing.

All the tyre samples were manufactured by the same manufacturer and the storage conditions were similar for all tyre samples before being mounted to the aircraft.

2.2 Preparation of specimens

The standard shape for each test method was obtained by standard dies and cutters. During the cutting process, the applied external forces were minimised as it adversely affected the tyre samples as polymers deform easily. Hence, all tyre samples were obtained only from the outermost layer (Fig. 1) of the tyre as it was the surface that was the most vulnerable to wear, unlike neither of the inner layers of the tyre. It was assumed that deformations did not happen in the process of obtaining the samples with the aid of dies and cutters.

As shown in Fig. 2, samples were obtained from each tyre sample having different shapes.

2.3 Labelling system for tyre samples

In order to identify tyre samples separately, each tyre and also each tyre sample was given a specific label. The tyre number and the sample number from each tyre were used in this tyre
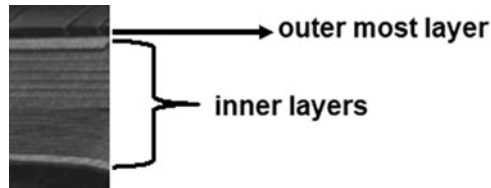
Figure 1. Cross-section of an aircraft tyre.

Figure 2. (Colour online) Standard shape types for tyre specimens; (a) Dumbbell shape;
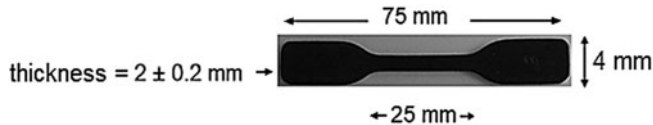(b) Rectangular; (c) Circular shape.

Figure 3. Dimensions of the test specimen.

sample labelling system. Hence, each tyre label gave a clear indication of the tyre number of a particular tyre sample belongs to and also the sample number in which sample that it belongs to in a particular tyre type. Four samples were obtained from each tyre for each test method. The labelling system for tested specimens was as follows:

Where if it was, XC_Y, X denoted the tyre number and Y denote the specimen number in each tyre. X = 0, 1, 2 and 3, Y = 1, 2, 3 and 4.

2.4 Material characterisations

All the tests were carried out as per ISO standards. The Uniaxial tensile test was carried out according to ISO 37 (5th edition, 2011-12-15) test standards, Abrasion test was done as per the ISO 4649 (3rd edition, 2010-09-15) and ISO 7619-1 (2nd edition, 2010-10-01) was followed for Hardness test.

2.4.1 Uniaxial tensile test and elongation test

The dumbbell shape test specimens were obtained (Fig. 3) after conditioning under the standard conditions as per the ISO 37 (5th edition, 2011-12-15) standard. The test samples comprised with the length of 25 mm, width 4 mm and thickness 2 mm.

As shown in Fig. 4, the thickness of each specimen was measured using Absolute Digimatic Indicator ID-C Series 543, Mitutoyo -Japan and recorded.

The clamping positions of each sample was marked using a sticky tape as shown in Fig. 5).

Each sample was mounted to the Tensometer (4486, Instron, US) individually as shown in Fig. 6 and the proper alignment of the laser beam was maintained along the centre of the sample.

Figure 4. (Colour online) Measuring the thickness of each sample.

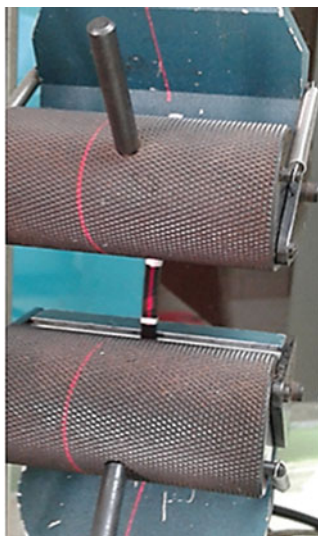Figure 5. (Colour online) Clamping positions in each sample.

Figure 6. (Colour online) Proper alignment of the beam along the centre of the sample.
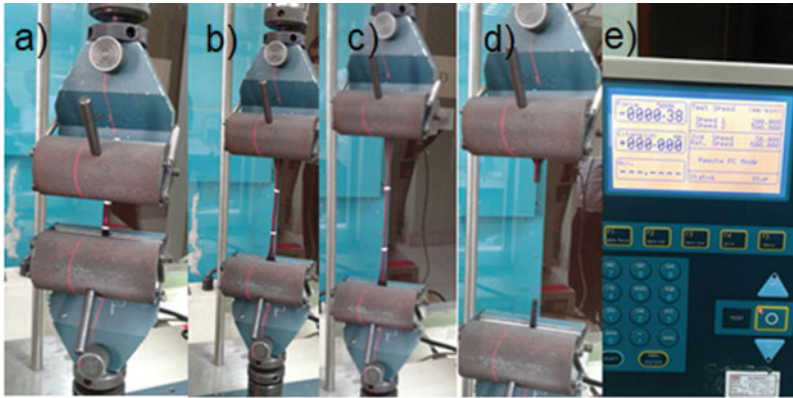
Figure 7. (Colour online) Sample testing in Tensometer (a) initial position, (b) elongation, (c) further elongation, (d) breakage, (e) recording.
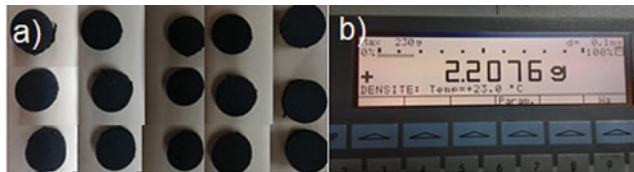

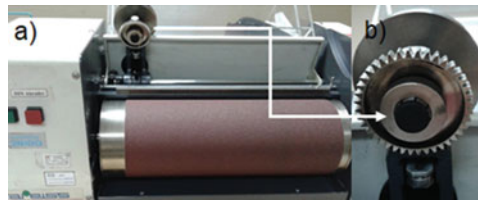Figure 8. (Colour online) Samples used for the abrasion test; (a) Sample specimens; (b) Weight recorder.

Figure 9. (Colour online) Abrader machine with the clamped sample; (a) Abrader machine; (b) Mounted circular tyre sample.

The Tensometer was operated in order to apply a force to the specimen. The respective elongations were recorded for each sample as shown in Fig. 7.

2.4.2 Abrasion test

After obtaining all the circular shape specimens (Fig. 8(a)) from both Control and Sample tyres the initial weights were measured (Fig. 8(b)) in every specimen using Sartorius, Analytical Balance-Germany and recorded.

The weighted specimen was clamped to the abrader machine (Fig. 9(a)) (HT8621B, Hung Ta Instruments, US) as shown in Fig. 9(b) and ISO 4649 (3rd edition, 2010-09-15) standard was followed to conduct the experiment.

The final weight for each specimen was recorded after each test as shown in Fig. 10.

The volume loss was calculated based on the weight difference.

Figure 10. (Colour online) Measuring the weight of specimen; (a) before the abrasion test;
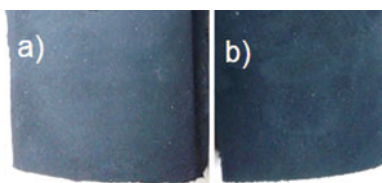(b) after the abrasion test.

Figure 11. (Colour online) Specimens for hardness test; (a) Control tyre sample;
(b) Worn-out tyre sample.

2.4.3 Hardness test

After obtaining all rectangular-shape specimens (Fig. 11) from the tyres, the Hardness test was carried out for each specimen after clamping the specimen in the hardness tester as shown in Fig. 12. The experiments were carried out as per ISO 7619-1 (2nd edition, 2010-10-01).

The obtained hardness values for each specimen was recorded.

3.0 RESULTS AND DISCUSSION

3.1 Tensile strength and elongation test results

The dimensions of a tested samples were shown in Fig. 3. The dimensions given in Table 1 are compatible with the standard dimensions given in ISO 37 (5th edition, 2011-12-15).

3.1.1 Dimensions for dumbbell specimens

Table 1 shows the dimensions of all the tested samples for tensile stress and strain. There were 24 dumbbell shaped specimens from three different tyre categories. Namely, $0C_1$, $0C_2$, $0C_3$ and $0C_4$ belong to all control tyre samples, which were obtained from each tyre types. The
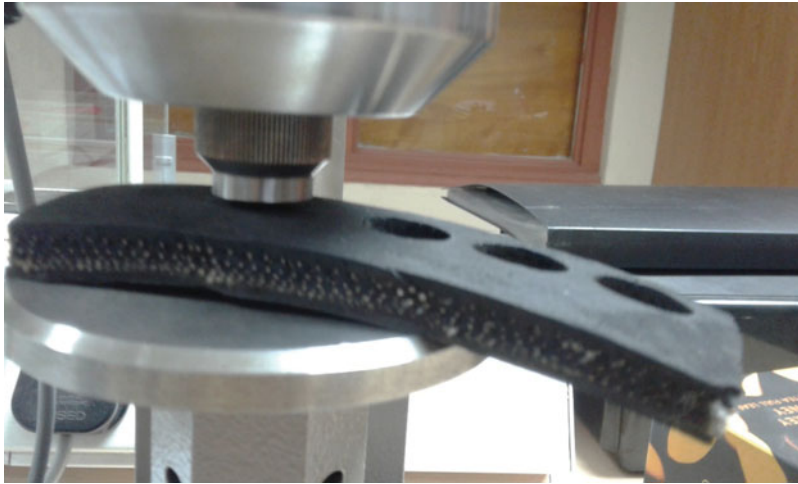
Figure 12. (Colour online) Clamped sample for hardness test.

notation of $1C_1$, $1C_2$, $1C_3$ and $1C_4$ belong to tyre type 1; $2C_1$, $2C_2$, $2C_3$ and $2C_4$ belongs to tyre type 2; and $3C_1$, $3C_2$, $3C_3$ and $3C_4$ belongs to tyre type 3. As per the values given in the table, the length and width were similar in all the dumbbell shapes. Although there was a small deviation of the thickness in each sample, these deviations were within the acceptable range as the deviated range of the width was ± 0.274 mm. Therefore, during the test, the dumbbell-shaped specimens were considered as uniform in dimensions.

3.1.2 Calculated values for tensile strength and elongation at break, %

As shown in Table 2, tensile strength values were calculated (Equation 1) for the specimens obtained from Tyre 1. Four readings were obtained for both Control tyre 1 and Sample tyre 1. The median tensile strength was calculated and the similar procedure was repeated for the other tyre types as well.

$$\text{Tensile strength} = (\text{applied load at break}) / (\text{original width}) \times (\text{original thickness}),$$
$$\dots (1)$$

$$\text{Percent elongation at break} = (\text{elongation at rupture}) \times 100 / (\text{initial gauge length})$$
$$\dots (2)$$

Similarly, the percentage of the elongation at break was also calculated (Equation 2) for each sample and the median value for the elongation was obtained for each tyre type.

When we consider the median tensile strength for the Control tyre samples obtained from Tyre 1, was 28.3 MPa and the median tensile strength for the Sample tyre 1 was 20.1 MPa. The percentages for the median elongation at break for Control tyre 1 and Sample tyre 1 were 240 and 224, respectively.

Similarly, Table 3 shows the tensile strength and elongation at break percentage for Tyre 2. When we consider Tyre 2, the median tensile strength for the control tyre samples obtained from Tyre 2, was 26.4 MPa and the median tensile strength for the Sample tyre 2 was 22.5 MPa. The percentages for the median elongation at break for Control tyre 2 and Sample tyre 2 were 235 and 229, respectively.

Table 1
Dimensions for the tested specimens

Sample	Tyre 1								Tyre 2								Tyre 3							
	Control tyre sample				Tyre sample 1				Control tyre sample				Tyre sample 2				Control tyre sample				Tyre sample 3			
Specimen identification	$0C_1$	$0C_2$	$0C_3$	$0C_4$	$1C_1$	$1C_2$	$1C_3$	$1C_4$	$0C_1$	$0C_2$	$0C_3$	$0C_4$	$2C_1$	$2C_2$	$2C_3$	$2C_4$	$0C_1$	$0C_2$	$0C_3$	$0C_4$	$3C_1$	$3C_2$	$3C_3$	$3C_4$
Median thickness (mm)	2.034	1.998	1.985	2.104	2.123	2.134	2.124	2.003	2.004	1.994	1.996	2.104	2.078	2.158	2.029	2.043	2.014	1.989	1.992	2.004	2.154	2.034	2.167	2.266
Width (mm)												4.00												
Length (mm)												75.00												

Table 2
**Median tensile strength values and median percentage of elongation
at break values for Tyre 1**

Sample	Control tyre 1				Sample tyre 1			
Specimen identification	$0C_1$	$0C_2$	$0C_3$	$0C_4$	$1C_1$	$1C_2$	$1C_3$	$1C_4$
Tensile strength (MPa)	28.5	28.3	28.3	28.1	20.1	20.0	20.1	21.2
Median tensile strength (MPa)		28.3				20.1		
Elongation at break, %	239	240	240	242	224	225	224	222
Median elongation at break, %		240				224		

Table 3
**Median tensile strength values and median percentage of elongation
at break values for tyre 2**

Sample	Control tyre 2				Sample tyre 2			
Specimen identification	$0C_1$	$0C_2$	$0C_3$	$0C_4$	$2C_1$	$2C_2$	$2C_3$	$2C_4$
Tensile strength (MPa)	26.4	27.3	26.4	25.1	22.5	22.0	22.5	22.6
Median tensile strength (MPa)		26.4				22.5		
Elongation at break, %	231	235	236	235	227	229	230	229
Median elongation at break, %		235				229		

Table 4
**Median tensile strength values and median percentage of elongation
at break values for tyre 3**

Sample	Control tyre 3				Sample tyre 3			
Specimen identification	$0C_1$	$0C_2$	$0C_3$	$0C_4$	$3C_1$	$3C_2$	$3C_3$	$3C_4$
Tensile strength (MPa)	28.7	28.5	28.5	28.1	20.0	19.8	19.9	19.9
Median tensile strength (MPa)		28.5				19.9		
Elongation at break, %	240	239	238	239	214	216	218	216
Median elongation at break, %		239				216		

As given in Table 4, the median tensile strength for the Control tyre samples obtained from Tyre 3 was 28.5 MPa and the median tensile strength for the Sample tyre 3 was 19.9 MPa. The percentages for the median elongation at break for Control tyre 3 and Sample tyre 3 were 239 and 216, respectively.
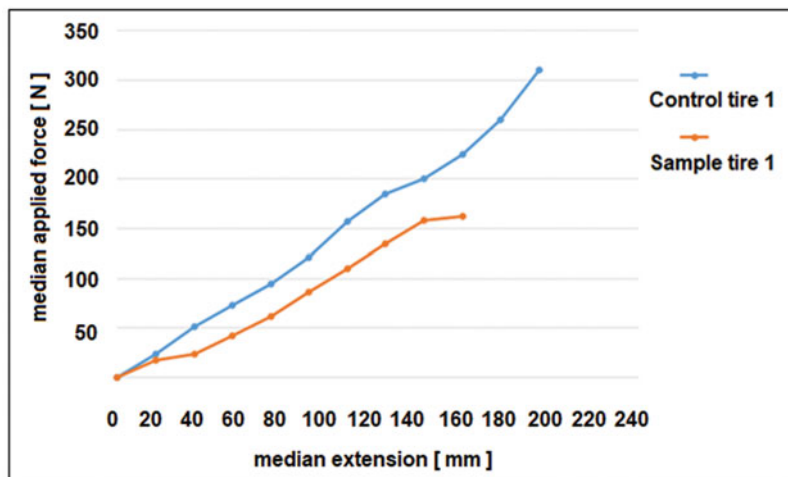
Figure 13. (Colour online) Median applied force vs median extension curves for Tyre 1.
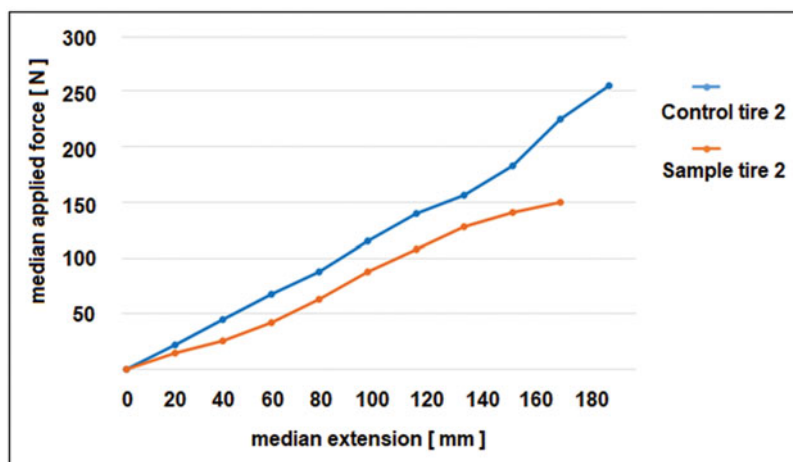

Figure 14. (Colour online) Median applied force vs median extension curves for Tyre 2.

3.1.3 Median applied force vs median extension curves

Figure 13 illustrates the variation of the median applied force under the increment of median extension for Tyre 1. As per the obtained trend of the curve, the median applied force was increasing while increasing the median extension for the sample. When the median applied force reached 310 N, Control tyre 1 obtained its median ultimate extension of 200 mm. Further extension caused the sample to break, as shown in Fig. 13. Sample tyre 1 achieved the highest median extension at 168 mm and the corresponding median applied force is 162 N, as shown in Fig. 13 below.

Figure 14 illustrates the variation of the median applied force under the increment of median extension for Tyre 2. When the median applied force reached 255 N, Control tyre 2 obtained its median ultimate extension of 180 mm. Sample tyre 2 achieved the highest
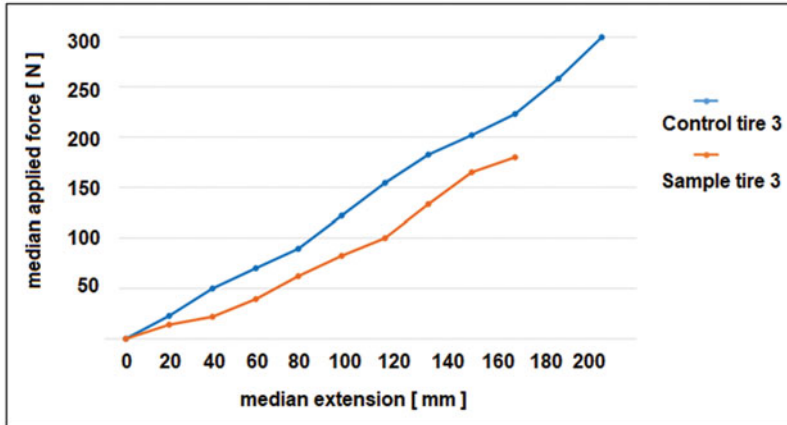
Figure 15. (Colour online) Median applied force vs median extension curves for Tyre 3.
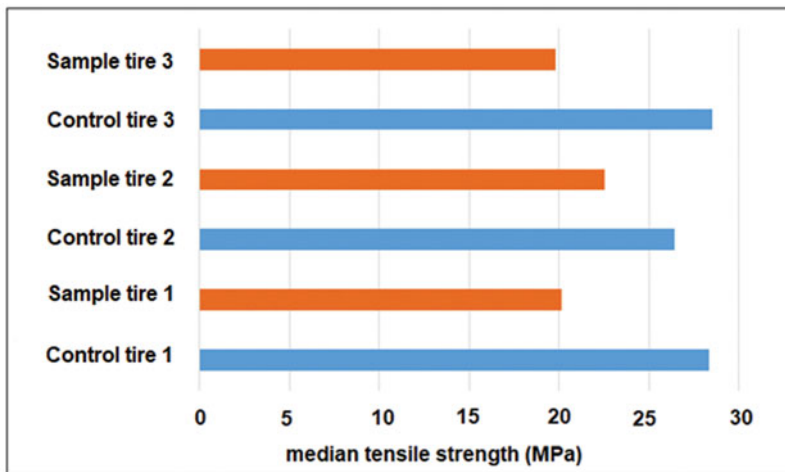

Figure 16. (Colour online) Comparison of median tensile strengths in each tested tyre sample.

median extension at 168 mm and the corresponding median applied force is 150 N, as shown in Fig. 14. Further extension of the samples caused the tyre samples to break.

Figure 15 below illustrates the variation of the median applied force under the increment of median extension for Tyre 3. When the median applied force reached 300 N, Control tyre 3 obtained its median ultimate extension of 200 mm. Sample tyre 3 achieved the highest median extension at 168 mm and the corresponding median applied force is 180 N. Further extension caused the tyre samples to break.

3.1.4 Comparison of median tensile strength and median elongation

Figure 16 illustrates the summary of median tensile strengths achieved by tyre samples in each tyre type against the respective control tyres. But out of three Control tyre samples, Tyre 1 and Tyre 3 showed similar and the highest median tensile strength values compared with the Control sample in tyre 2. In addition, after the completion of 50 landings, the highest
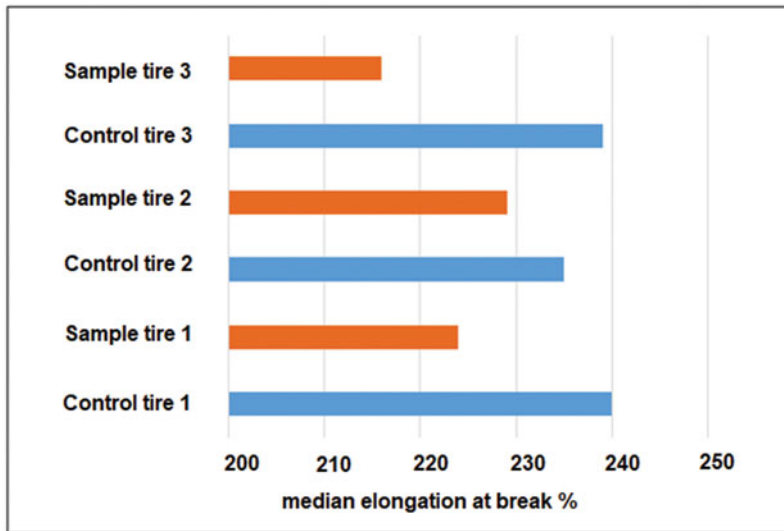
Figure 17. (Colour online) Comparison of median elongation at break for each tyre sample.

Figure 18. Dimensions of the specimen for Abrasion test.

median tensile strength could be seen for Sample tyre 2 when compared with Tyre 1 and Tyre 3. Moreover, similar median tensile strength could be observed in Tyre 1 and Tyre 3 after the completion of 50 landings.

Figure 17 shows the comparison of median elongation at break for each tyre type. The highest median elongation at break was reported for Control tyre samples when compared with tyre samples that had completed 50 landings.

3.2 Abrasion test

3.2.1 Dimensions of the specimens for Abrasion test

Circular-shaped specimens (Fig. 18) were obtained from each tyre sample using a standard cutter. Hence, all the dimensions for 24 specimens could be assumed to be similar.

3.2.2 Measurements for the specimens after Abrasion test

According to the data given in Table 5, the weight losses for the specimens obtained from Tyre 1 were calculated by considering the initial weight of each specimen and the final weight of each specimen after the Abrasion test was carried out. In addition, the rotational speed of the abrader machine was taken as 200 times/min.

Based on Equation (3), the weight loss with respect to the reference material was calculated and the resulting values are shown in Table 5.

$$Wrs = (\Delta\,Ws/Wr)\,\times 200 \qquad\qquad …\,(3)$$

Table 5
Weight loss of each specimen for Tyre 1 in Abrasion test

Sample	Control tyre 1				Sample tyre 1			
Specimen identification	$0C_1$	$0C_2$	$0C_3$	$0C_4$	$1C_1$	$1C_2$	$1C_3$	$1C_4$
Weight loss, (ΔWs) mg	156.83	156.93	156.88	157.70	153.50	149.90	154.20	148.10
Weight loss w.r.t reference material, (Wrs)	146.09	146.19	146.14	146.90	142.99	139.63	143.64	137.96
Volume loss mm^3 (Wrs/D)	127.84	127.92	127.88	128.54	125.12	122.18	125.69	120.72
Mean Volume loss mm^3		128.05				123.43		

Table 6
Weight loss of each specimen for Tyre 2 in Abrasion test

Sample	Control tyre 2				Sample tyre 2			
Specimen identification	$0C_1$	$0C_2$	$0C_3$	$0C_4$	$2C_1$	$2C_2$	$2C_3$	$2C_4$
Weight loss, (ΔWs) mg	158.02	157.75	156.90	157.15	156.50	147.90	152.90	153.80
Weight loss w.r.t reference material, (Wrs)	147.20	146.95	146.16	146.39	145.78	137.77	142.43	143.26
Volume loss mm^3 (Wrs/D)	128.81	128.59	127.90	128.10	127.56	120.55	124.63	125.36
Mean volume loss mm^3		128.35				124.53		

$$\text{Volume loss} = Wrs/D \qquad \dots (4)$$

The mean density (D) for the tyre sample was taken as 1.1428 g/cm^3 and the weight of the reference sample (Wr) was taken as 214.7 mg for the calculation. The ISO 4649 standard was followed even for the reference material.

By substituting the calculated values of Equation (4), the volume loss was calculated for each specimen and the mean volume loss was also calculated for each tyre type. Similar calculation method was applied for the data given in Tables 6 and 7 which are related to Tyre 2 and Tyre 3.

As given in Table 5, the mean volume loss for the control sample obtained from Tyre 1 was 128.05 mm^3. The mean volume loss for Sample tyre 1 was 123.43 mm^3.

Table 7
Weight loss of each specimen for Tyre 3 in Abrasion test

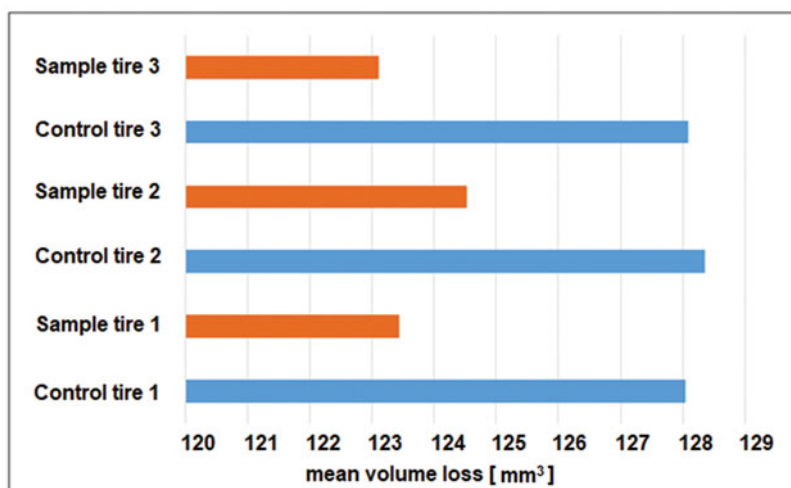| Sample	Control tyre 3				Sample tyre 3			
Specimen identification	$0C_1$	$0C_2$	$0C_3$	$0C_4$	$3C_1$	$3C_2$	$3C_3$	$3C_4$
Weight loss, (ΔWs) mg	157.06	157.13	156.99	157.33	150.50	148.90	151.90	152.80
Weight loss w.r.t reference material, (Wrs)	146.31	146.37	146.24	146.56	140.20	138.71	141.50	142.34
Volume loss mm^3 (Wrs/D)	128.03	128.08	127.97	128.25	122.68	121.38	123.82	124.55
Mean volume loss mm^3	128.08				123.11			

Figure 19. (Colour online) Comparison of the mean volume loss for each tyre type.

As shown in Table 6, the mean volume loss for the control sample obtained from Tyre 2 was $128.35 \, mm^3$ and the mean volume loss for Sample tyre 2 was $124.53 \, mm^3$.

According to the Table 7, $128.08 \, mm^3$ of the mean volume loss was achieved by the Control tyre 3 sample while the corresponding Sample tyre 3 obtained $123.11 \, mm^3$ of the mean volume loss.

3.2.3 Comparison of the mean volume loss

According to Fig. 19, the maximum mean volume loss was shown in Tyre 3 and the minimum mean volume loss was observed in Tyre 2. Seemingly, Tyre 1 shows similar mean volume loss to Tyre 3.
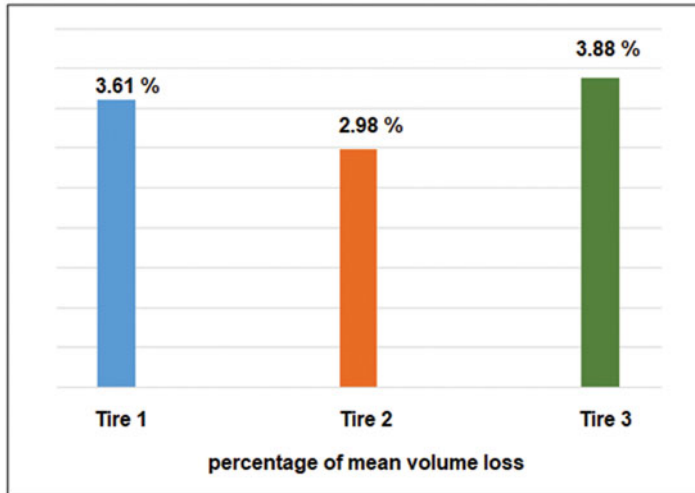
Figure 20. (Colour online) Comparison of percentage of mean volume loss.

Figure 20 illustrates the percentage of mean volume loss in each tyre type compared to its Control tyre. Similar to the results obtained in Fig. 19, the maximum percentage of mean volume loss was achieved by Tyre 3 and it was 3.88% after the completion of 50 landings while the percentage of mean volume loss was 3.61% for Tyre 1. The least percentage of mean volume loss occurred in Tyre 2, which was 2.98% after 50 landings.

3.3 Hardness test

3.3.1 Dimensions of the specimens for the Hardness test

As per ISO 7619-1 (2nd edition, 2010-10-01), the thickness of each specimen should be greater than 6.00 mm for the Hardness test. The average thickness for each tested tyre sample is given in Table 8 below.

According to the sample thickness values given in Table 8, all the sample thickness values were above the required minimum value for the thickness.

3.3.2 Measurements for hardness

As given in Table 9, the median hardness values of Tyre 1 was 61.5 Shore A for Control tyre 1 and 58.8 Shore A for Sample tyre 1. Similarly, the median hardness values of Tyre 2 was 59.2 Shore A for Control tyre 2 and 55.1 Shore A for Sample tyre 2. In addition, Tyre 3 demonstrated 61.7 Shore A median hardness values for its Control tyre 3 while Sample tyre 3 was measured at 58.6 Shore A hardness.

3.3.3 Comparison of hardness

As shown in Fig. 21, hardness was dropped in all tyre types after the completion of 50 landings. However, the reduction of hardness in Tyre 1 and Tyre 3 looks similar.

Figure 22 shows the percentage of hardness reduction in each tyre type after the completion of 50 landings. The hardness reduction percentage was 4.4% for Tyre 1 and 5.0% for Tyre 3. The highest hardness reduction percentage was obtained for Tyre 2 with a value of 6.9%.

Table 8
Thickness of tyre samples used for the Hardness test

Sample	Tyre 1								Tyre 2								Tyre 3							
	Control tyre 1				Sample tyre 1				Control tyre 2				Sample tyre 2				Control tyre 3				Sample tyre 3			
Specimen identification	$0C_1$	$0C_2$	$0C_3$	$0C_4$	$1C_1$	$1C_2$	$1C_3$	$1C_4$	$0C_1$	$0C_2$	$0C_3$	$0C_4$	$2C_1$	$2C_2$	$2C_3$	$2C_4$	$0C_1$	$0C_2$	$0C_3$	$0C_4$	$3C_1$	$3C_2$	$3C_3$	$3C_4$
Thickness (mm)	12.2	12.3	12.5	12.1	12.5	12.3	12.6	12.2	12.4	12.3	12.6	12.0	12.1	12.6	12.8	12.4	12.5	12.1	12.2	12.3	12.2	12.7	12.9	12.3

Table 9
Hardness values for each specimen and the Median Hardness values

| Sample	Tyre 1								Tyre 2								Tyre 3							
	Control tyre 1				Sample tyre 1				Control tyre 2				Sample tyre 2				Control tyre 3				Sample tyre 3			
Specimen identification	$0C_1$	$0C_2$	$0C_3$	$0C_4$	$1C_1$	$1C_2$	$1C_3$	$1C_4$	$0C_1$	$0C_2$	$0C_3$	$0C_4$	$2C_1$	$2C_2$	$2C_3$	$2C_4$	$0C_1$	$0C_2$	$0C_3$	$0C_4$	$3C_1$	$3C_2$	$3C_3$	$3C_4$
Hardness shore A	61.5	61.5	61.6	61.4	58.6	58.8	58.9	56.8	59.3	59.2	59.1	59.2	55.1	55.0	55.1	55.3	61.8	61.7	61.6	61.7	58.3	58.6	58.9	58.6
Median hardness shore A	61.5				58.8				59.2				55.1				61.7				58.6			
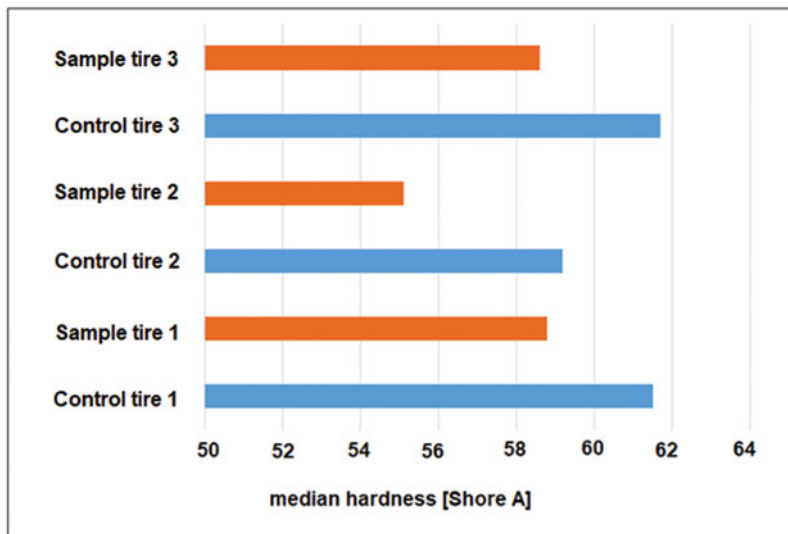
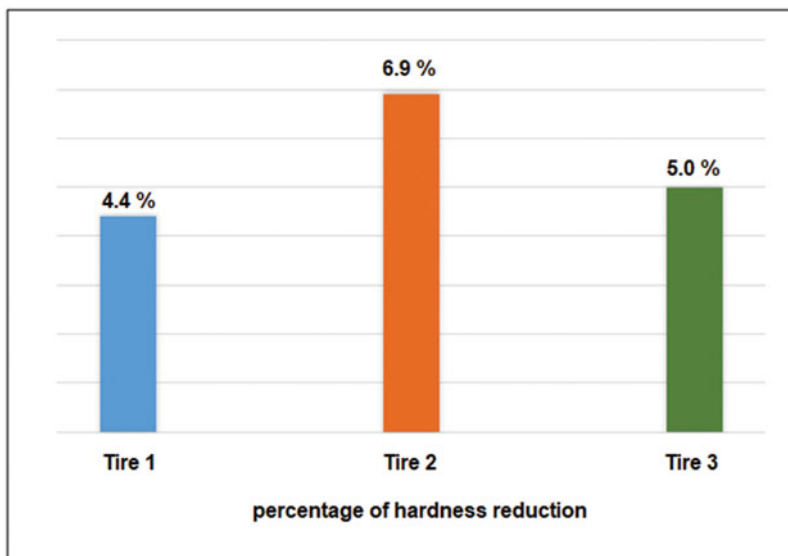Figure 21. (Colour online) Comparison of median hardness in each tyre type.

Figure 22. (Colour online) Comparison of percentage in hardness reduction.

3.4 Surface morphology of the samples

The physical appearance of the tyre samples was obtained using the Scanning Electron Microscope Hitachi SU 6600-Japan.

As shown in Fig. 23, there was a significant variation in the surface morphologies between the Control tyre sample and the worn-out tyre sample. The Control tyre sample showed smooth surface compared with the worn-out tyre sample.
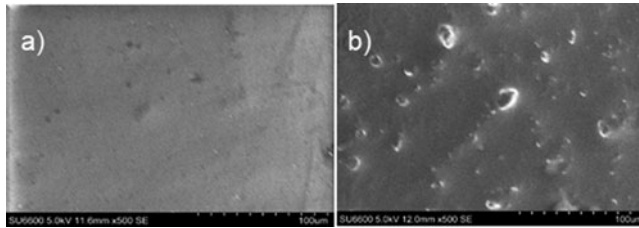
Figure 23. Surface Morphologies of the tyre samples; (a) Control tyre sample; (b) Worn-out tyre sample 1.

4.0 CONCLUSIONS

This study is a novel empirical approach solely for the Y12 aircraft tyres. The outcome of this study will be important for engineering practitioners, tyre manufacturers and researchers. The engineers could carry out the relevant Non Destructive Test (NDT) to Y12 aircraft tyres after the completion of 50 landings in the absence of visible micro-cracks and recommend the tyres for further usage without discarding them. The outcome of this research will be useful for aircraft tyre manufacturers and researchers to further develop existing Y12 aircraft tyres thusly to withstand a higher number of landings in the presence of cyclic compressed/uncompressed loads, shear stresses and strains. This research work related to determine the variation of polymeric properties in Y12 aircraft tyres which is also one of the key factors in nonlinearity parameters that deal with the thermomechanical behaviour of aircraft tyres. Hence, this study fills the gap of finding the polymeric properties of aircraft tyres which will important in thermomechanical analysis of aircraft tyres[15]. Three tyre samples were used for the experiment with one tyre from the nose wheel (Tyre 2), one tyre from left main gear (Tyre 1) and one tyre from right main gear (Tyre 3). There was a 29% of median tensile strength reduction in Tyre 1 and the reduction of the percentage of median elongation at was break reported as 6.6 for Tyre 1. The reduction of the percentages of both the median tensile strength and the elongation at break were 14.8 and 2.6, respectively, for Tyre 2. The median tensile strength reduction percentage was 30.2 for Tyre 3 while it recorded 9.6% of reduction of median elongation at break. As per the literature[16], the main gears touch down on the runway surface prior to the touchdown of the nose gear. The initial weight of the aircraft has to confront the main gear wheels[14]. Hence, the reduction of the percentages of median tensile strength and elongation at break were higher in Tyre 1 and Tyre 3 compared with Tyre 2, as Tyre 1 indicates the left main gear tyre and Tyre 3 indicates the right main gear tyre. The reduction of the percentage of median tensile strength and elongation at break was lower in Tyre 2 which represent the nose-gear tyre as it has to tackle only 10–12% from the weight of the aircraft while the main gear tyres have to bear 88–90% of the weight[14]. In addition, the percentage of mean volume loss were roughly similar in both Tyre 1 and Tyre 3, but those values were higher than the percentage of mean volume loss recorded for Tyre 2. These experimental results also concurred with the literature details as the nose-gear tyre has to bear the percentage of the lower amount of weight percentage from the aircraft compared with the main-gear tyres. Hence, the percentage of mean volume loss was higher for main-gear tyres compared with the nose-gear tyre. The highest percentage of hardness reduction was reported in Tyre 2, while other tyre types showed lower percentage of hardness reduction. The cross-section of the aircraft tyre consists with multiple layers[1,17] in order to make them more stronger. However, as the Y12 aircraft has a tricycle gear system, the main gear supports

most of the weight; therefore, it is the strongest compared with the nose gear. The roll of the nose gear is to prevent the nose of the aircraft from tipping down as the centre of gravity is forward of the main gear. In addition, the diameter of the nose gear tyre is smaller than the diameter of the main gear tyres. Further, this smaller-diameter tyre has to bear 10–12% from the weight of the aircraft, which causes it to wear down sooner than the tyres in the main gears. This could be the reason to have a higher percentage reduction in hardness for Tyre 2 than Tyre 1 and Tyre 3.

As according to the SEM micrographs there is a significant variation in the surface morphologies of the control tyre sample and worn out tyre samples, where the control tyre sample has a smooth surface while the worn-out tyre sample has a rough surface.

5.0 SUGGESTIONS

Further, analysis could be done to identify the property discrepancies in internal layers as well.

ACKNOWLEDGEMENTS

REFERENCES

1. Konde, A.K., Rosu, I., Lebon, F., Brardo, O. and Devesa, B. On the modeling of aircraft tire, *Aerospace Science and Technology J*, 2013, **27**, pp 67-75.
2. Behroozi, M., Olatunbosun, O.A. and Ding, W. Finite element analysis of aircraft tyre – Effect of model complexity on tyre performance characteristics, *Materials and Design J*, 2012, **35**, pp 810-819.
3. Guo, H., Bastien, C., Blundell, M. and Wood, G. Development of a detailed aircraft tyre finite element model for safety assessment, *Materials and Design J*, 2014, **53**, pp 902-909.
4. Alroqi, A.A. and Wang, W. Comparison of aircraft tire wear with initial wheel rotational speed, *Int J Aviation, Aeronautics and Aerospace*, 2015, **2**(1), pp 1-28.
5. Clark, S.K. and Dodge, R.N. Heat generation in aircraft tires, *J Computers & Structures*, 1985, **20**(1-3), pp 535-544.
6. Good Year Company. Aircraft tire care and maintenance, 2017. Available at: https://www.goodyearaviation.com/resources/pdf/aviation_tyre_care_3_2017.pdf (accessed 3 November 2017).
7. Kongo, K.A., Rosu, I., Ebon, F., Brardo, O. and Devesa, B. Study of the rolling behavior of an airplane tire, AIRBUS, 316 Bayonne Road, 31060 Toulouse cedex 03.
8. Tanner, J.A., Dreher, R.C., Strubb, S.M. and Smith, E.G. Tire tread temperatures during antiskid braking and cornering at dry runway, NASA Technical Paper 2009, 1982.
9. Mc Carthy, J.L. and Tanner, J.A. Temperature distribution in an aircraft tire at low ground speed, NASA Technical Paper 2195, 1983.
10. Clark, S.K. and Doge, R. N. Heat generation in aircraft tires under free rolling conditions, NASA Contractor Report 3629, 1982.
11. Konde, A.K., Rosu, I., Lebon, F., Brardo, O. and Devesa, B. Thermomechanical analysis of an aircraft tire in cornering using coupled ale and lagrangian formulations, *Central European J Engineering*, 2013, **3**(2), pp 191-205.
12. Hamid, M. and Ghoreishy, R. Finite element analysis of the steel-belted radial tyre with tread pattern under contact load, *Iranian Polymer J*, 2006, **15**(8), pp 667-674.
13. All the World's Aircraft. Available at: http://www.aviaMarchket.org/china/hai/y-12.html (accessed 15 January 2018).

14. Introduction to aeronautics: A design perspective, Chapter 7, pp 215-239. Available at: https://www.southampton.ac.uk/~jps7/Aircraft%20Design%20Resources/Brandt%20Introduction%20to%20Aeronautics/Ch7Structure.doc (accessed 20 January 2018).

15. RAFEI, M., GHOREISHY, M. H. R. and NADERI, G. Thermo-mechanical coupled finite element simulation of tire cornering characteristics - Effect of complex material models and friction law, *Mathematics and Computers in Simulation*, 2018, **144**, pp 35-51.

16. Federal Aviation administration. Aviation maintenance technician handbook- airframe, 2012, **2**. Available at: https://www.faa.gov/regulations_policies/handbooks_manuals/aircraft/amt_airframe_handbook/media/ama_Ch13.pdf (accessed 3 November 2017).

17. XIE, M., TANG, H. and YAO, H. Failure analysis of tire separation in two-sized tires on Airbus planes, *Engineering Failure Analysis J*, 2016, **61**, pp 21-27.